

Quark-hadron duality and Q^2 evolution of the GDH integral in the HERMES experiment

A. Fantoni^a

On behalf of the HERMES Collaboration
INFN - Laboratori Nazionali di Frascati, Frascati (Roma), Italy

Received: 1 November 2002 /

Published online: 15 July 2003 – © Società Italiana di Fisica / Springer-Verlag 2003

Abstract. First results on quark-hadron duality in the spin sector from the HERMES experiment are reported in the range $1.2 \leq Q^2 \leq 12 \text{ GeV}^2$ and $1 \leq W^2 \leq 4 \text{ GeV}^2$. A complete set of measurements of the generalised GDH integrals for the deuteron, proton and neutron is also shown in the same Q^2 range and in the full W^2 range.

PACS. 13.60.Hb Total and inclusive cross-sections (including deep-inelastic processes) – 12.38.Qk Experimental tests – 13.88.+e Polarization in interactions and scattering – 25.20.Dc Photon absorption and scattering

1 Introduction

The Bloom-Gilman duality [1] is a relation between the deep inelastic scattering (DIS) region and the resonance region in lepton hadron scattering. It states that the smooth scaling curve seen at high momentum transfer is an accurate average over the resonance bumps seen at lower momentum transfer, but at the same values of the Bjorken scaling variable x . This is a manifestation of the fact that the single-quark reaction rate determines the scale of the reaction rate for the entire process down to remarkably low energies and momentum transfers. An analysis of the resonance region in terms of QCD, which describes in a rigorous way the Q^2 -dependence of the unpolarised proton structure function F_2 at large photon-nucleon invariant mass squared W and Q^2 , was presented for the first time in [2]. The conclusion was that changes in the lower moments of the F_2 structure function due to higher-twist effects are small, so that averages of this function over a sufficient range in x at moderate and high values of the transferred momentum squared Q^2 are approximately the same. A recent discussion of the duality concept can be found in [3], where the term duality is used to describe the rare cases where the average of hadronic observables is described by a perturbative QCD (pQCD) calculation. In inelastic electron scattering as $Q^2 \rightarrow 0$ pQCD must fail. In fact, the breakdown in duality as $Q^2 \rightarrow 0$ can be seen from the impossibility of reproducing the neutron form factor at $Q^2 = 0$, *i.e.*, zero, from the sum of squares of the quark charges. Re-

cent results from JLab [4] have shown that duality in the unpolarised structure function F_2 for proton holds for individual resonance contribution as well as for the entire resonance region $1 \leq W^2 \leq 4 \text{ GeV}^2$, starting from values of $Q^2 \geq 1.5 \text{ GeV}^2$.

In contrast to the extensive study of duality for the unpolarised, *i.e.* spin-averaged, photo-absorption cross-section, the validity of duality has not been investigated for the spin-dependent scattering processes, which are related to the spin-*dependent* photo-absorption cross-section. Even though duality was observed for the unpolarised structure functions, there is no *a priori* reason to believe that duality also holds for polarised structure functions. In fact, duality is expected to fail for polarised structure functions at low Q^2 , since for the proton the Ellis-Jaffe sum rule and the Gerasimov-Drell-Hearn sum rule (at $Q^2 = 0$) are positive and negative, respectively [5]. The interest for the duality in the polarised case started recently [6]. At the moment, no information is available on the possible quark-hadron duality in the spin sector. Results on the proton target are shown in sect. 2.2.

Data obtained in the resonance region have been used in combination with the analysis at higher W^2 to provide the Q^2 evolution of the Gerasimov-Drell-Hearn (GDH) integral for the proton, neutron and deuteron. The GDH sum rule [7] is derived starting from a general dispersive relation for the forward Compton scattering, which follows causality, crossing symmetry and unitarity principles. It relates the anomalous contribution in the nucleon magnetic moment κ to an energy-weighted integral of the difference of the nucleon's total spin-dependent

^a e-mail: alessandra.fantoni@lnf.infn.it

photo-absorption cross-section:

$$\int_{\nu_0}^{\infty} \frac{d\nu}{\nu} [\sigma_{1/2}(\nu) - \sigma_{3/2}(\nu)] = -\frac{2\pi^2\alpha}{M^2} \kappa^2,$$

where ν is the photon energy, ν_0 is the photo-absorption threshold, M is the nucleon mass and $\sigma_{1/2}$ and $\sigma_{3/2}$ are the absorption cross-sections for total helicity 1/2 and 3/2. The sum rule defined is based on the additional assumptions of the low-energy theorems and the no-subtraction hypothesis for the spin-flip part of the Compton scattering amplitude. It provides an interesting link between the helicity-dependent dynamics and a static ground property of the target nucleus and it holds for any type of target. The previous expression is valid for nucleon target (spin 1/2) and will be slightly modified for nuclear target. The GDH integral can be generalised to the case of absorption of polarised transverse virtual photons,

$$\begin{aligned} I(Q^2) &= \int_{Q^2/2M}^{\infty} [\sigma_{1/2}(\nu, Q^2) - \sigma_{3/2}(\nu, Q^2)] \frac{d\nu}{\nu} \\ &= \frac{8\pi^2\alpha}{M} \int_0^{x_0} \frac{g_1(x, Q^2) - \gamma^2 g_2(x, Q^2)}{K} \frac{dx}{x}, \end{aligned}$$

where g_1 and g_2 are the polarised structure functions of the nucleon, $x_0 = Q^2/2M\nu_0$ and K is the flux factor of virtual photons, defined as $\nu\sqrt{1+\gamma^2}$ in the Gilman notation [8], with $\gamma^2 = Q^2/\nu^2$. For the real-photon case, when $Q^2 = 0$ (GDH value), the integral reduces to the GDH sum rule, while for the high-energy limit (DIS), when $\gamma \ll 1$, the integral becomes

$$I(Q^2) = \frac{16\pi^2\alpha}{Q^2} \int_0^{x_0} g_1(x) dx = \frac{16\pi^2\alpha}{Q^2} \Gamma,$$

where Γ is the first moment of $g_1(x)$. Thus the generalised GDH integral provides a way to study the transition from polarised real-photon absorption ($Q^2 = 0$) on the nucleon to polarised deep inelastic scattering, that is the transition from non-perturbative regime at low Q^2 to the perturbative regime at high Q^2 . Results on the proton, neutron and deuteron targets are shown in sect. 3.

2 Duality: analysis procedure

The data were collected by the HERMES experiment in 1997 with 27.56 GeV longitudinally polarised positron beam incident on a longitudinally polarised ^1H gas target internal to the HERA storage ring at DESY. Scattered positrons were detected by the HERMES spectrometer [9]. The kinematic requirements on the scattered positrons for the analysis in the nucleon resonance region were $1 \leq W^2 \leq 4 \text{ GeV}^2$ and $1.2 \leq Q^2 \leq 12 \text{ GeV}^2$, with the corresponding x in the range $0.34 < x < 0.98$. After applying data quality criteria, about 120000 events remained.

The evaluation of the measured longitudinal asymmetry A_{\parallel} is based on the ratio of weighted count rates according to the formula $A_{\parallel} = (N^-L^+ - N^+L^-)/(N^-L_p^+ +$

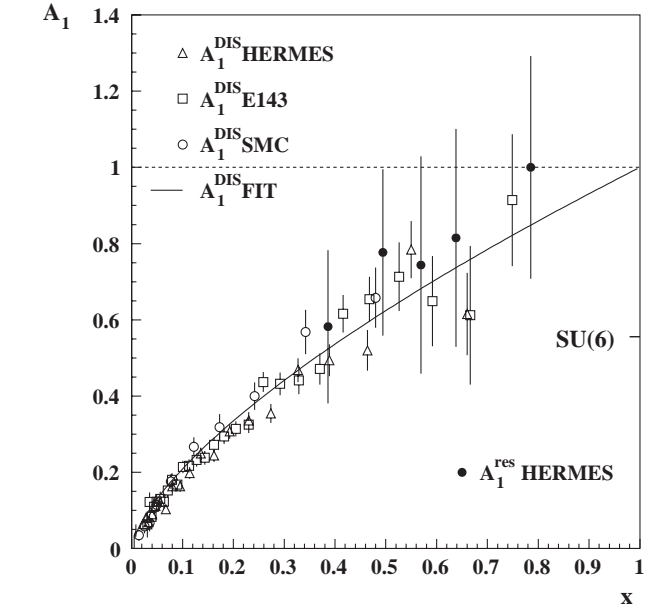


Fig. 1. Spin asymmetry A_1 as a function of x . The curve represents a fit to DIS data at large x .

$N^+L_p^-)$, where N is the number of detected scattered positrons, L is the integrated luminosity corrected for dead time, L_p is the integrated luminosity corrected for dead time and weighted by the product of the beam and target polarisations. The superscript + (−) refers to the situation where the target spin axis was oriented parallel (anti-parallel) to that of the positron beam.

The limited W resolution in the resonance region ($\delta W \approx 240 \text{ MeV}$) does not allow individual nucleon resonances to be distinguished or the DIS and resonance regions to be completely separated. To evaluate the smearing correction and the contaminations in the resonance region from the elastic and deep inelastic regions, these effects were studied using a simulation of events from elastic, resonance and deep inelastic processes. The parameterisations of these contributions were taken from refs. [10–12]. The “true” value of $A_{\parallel}^{\text{res}}$ is obtained from the relation $A_{\parallel}^{\text{meas}} = A_{\parallel}^{\text{res}} f_{\text{res}} + A_{\parallel}^{\text{DIS}} f_{\text{DIS}} + A_{\parallel}^{\text{el}} f_{\text{el}}$, where $f_{\text{el},\text{res},\text{DIS}}$ denote the contaminations from corresponding kinematic regions to the resonance one. The contamination from elastic and DIS events in the resonance region varies from 9% to 3.8% and from 10% to 18.5%, respectively, with Q^2 ranging from 1.2 to 12 GeV^2 .

2.1 The spin asymmetry A_1

The virtual photo-absorption asymmetry A_1 was extracted from the measured longitudinal asymmetry A_{\parallel} using the relation $A_1 = A_{\parallel}/D - \eta A_2$, where D is the virtual photon depolarisation factor and η is a kinematic factor. The contribution of the asymmetry A_2 is taken into account as $A_2 = 0.06 \pm 0.16$ as obtained from SLAC [13] at $Q^2 = 3 \text{ GeV}^2$. In fig. 1 the spin asymmetry in the nucleon resonance region A_1^{res} is shown as a function of x . For

each value of x the quantity A_1^{res} has been averaged over Q^2 . The total systematic uncertainty of the data is about 16% with the dominant contribution originating from A_2 amounting to 14%. The extracted spin asymmetry A_1^{res} increases with x . The data indicate that A_1^{res} may exceed the $SU(6)$ prediction of $5/9$ at $x = 1$. As is seen, the A_1 measured in the resonance region is in agreement within the experimental error with previous DIS data at higher Q^2 and W^2 . The curve is a fit on world DIS data at $x > 0.3$, $A_1 = x^{0.68}$. This parameterisation of A_1 is constraint to 1 at $x = 1$ and does not depend on Q^2 . The average ratio of the measured A_1^{res} to the DIS fit is $1.15 \pm 0.16 \pm 0.18$. This suggests that the description of the spin asymmetry in terms of quark degrees of freedom is also valid in the nucleon resonance region for the Q^2 range explored by the present experiment [14].

2.2 Q^2 -dependence of duality in the structure function g_1

The verification of the quark-hadron duality can be obtained comparing the integrals of the polarised structure function g_1 in the resonance and DIS region in the same x interval. The integrals $\Gamma_1 = \int_{x_{\text{min}}}^{x_{\text{max}}} g_1(x) dx$ have been evaluated separately for the resonance and DIS domains. For each Q^2 bin the integral Γ_1^{res} has been calculated using the relation $g_1(x) = A_1^{\text{res}} \cdot F_1(x)$ to account for the x -dependence of the integrand F_1 within the individual x bins. The unpolarised structure function $F_1 = F_2(1 + \gamma^2)/(2x(1 + R))$ was calculated from a modification of the parameterisation [11] of F_2 that accounts for nucleon resonance excitation and assuming $R = 0.18$ in the whole W^2 region considered. The limits of integration x_{max} and x_{min} were calculated in each Q^2 bin from the W_{min}^2 and W_{max}^2 , respectively. The integral Γ_1^{DIS} was calculated in the same x range and at the same Q^2 values as for Γ_1^{res} . The value of A_1^{DIS} was taken from the Q^2 -independent fit to DIS data at large x , the unpolarised structure function F_2 was taken from ref. [12], and the value of R from ref. [15]. The ratio $\Gamma_1^{\text{res}}/\Gamma_1^{\text{DIS}}$ for several Q^2 values is shown in fig. 2, together with the values from SLAC, evaluated by dividing the measured value of Γ_1^{res} [13] by Γ_1^{DIS} calculated in the same way as for the present data. The Bjorken variable x is sometimes replaced by the Nachtmann variable $\xi = 2x/(1 + \sqrt{1 + \gamma^2})$ [16], which includes the target mass corrections. For high Q^2 , ξ approaches x , which is the scaling variable at large Q^2 . The ratio $\Gamma_1^{\text{res}}/\Gamma_1^{\text{DIS}}$ using the Nachtmann variable ξ as integration variable is also shown in fig. 2. No large effects due to target mass corrections are observed.

3 The generalised GDH integral

The kinematic of the HERMES experiment allows to study the Q^2 -dependence of the generalised GDH integral simultaneously in the nucleon resonance and DIS region. The full range in W^2 ($1.0 < W^2 < 45 \text{ GeV}^2$) was

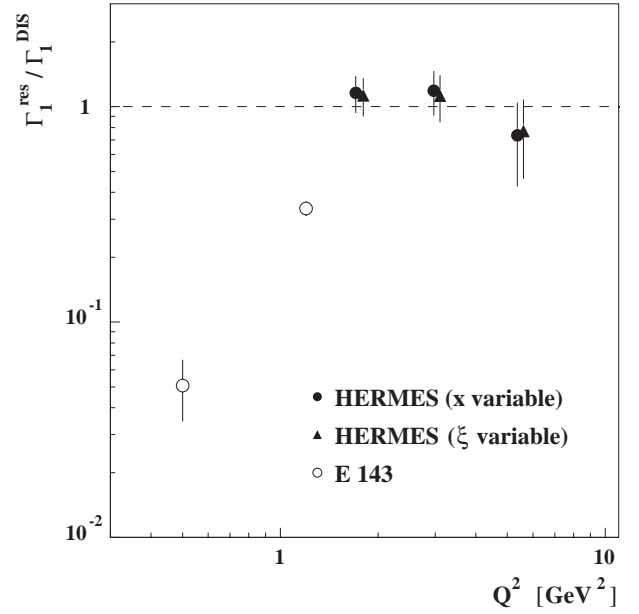


Fig. 2. Ratio between Γ_1 in the resonance region and Γ_1 in the DIS region as a function of Q^2 . The data are shown using x (full circles) or ξ (full triangles) as integration parameter. Points in ξ are slightly shifted to make them more visible.

separated into nucleon resonance region ($1.0 < W^2 < 4.2 \text{ GeV}^2$) and DIS region ($4.2 < W^2 < 45.0 \text{ GeV}^2$). The Q^2 range $1.2 < Q^2 < 12.0 \text{ GeV}^2$ was divided into six bins. Results are shown for proton, neutron and deuteron targets. HERMES data on the deuteron target were taken in 1998 to 2000. After applying data quality criteria, 0.55 (0.13) million events on the deuteron (proton) in the nucleon resonance region and 8.3 (1.4) million events in the DIS region were selected.

The analysis procedure for the resonance region is the same as in sect. 2.2, while the analysis for the DIS region has been described in [17]. Results on the generalised GDH integral for the proton have been published previously [18]. Proton data have been used together with deuteron data to obtain the neutron data. In fact, the integral I_{GDH}^n for the neutron was calculated from the results I_{GDH}^d on the deuteron and those on the proton I_{GDH}^p , following the relation $I_{\text{GDH}}^n = I_{\text{GDH}}^d/(1 - 1.5\omega_d) - I_{\text{GDH}}^p$, where ω_d [19] is the probability of the deuteron to be in a D -state.

The results of $I_{\text{GDH}}^{\text{res}}$ for the p , n and d targets are presented in fig. 3. The integrals strongly decrease (in absolute value) with Q^2 and become negligible for $Q > 3 \text{ GeV}^2$. The integrals are compared to a model [20] which describes the resonance excitation in the approximation of infinitely narrow resonances and includes a contribution from one-pion exchange in the near-threshold region. This model is not sufficient to well reproduce the experimental results for $Q < 2 \text{ GeV}^2$. In the plot, statistical and systematic uncertainties are shown together.

The results of $I_{\text{GDH}}^{\text{DIS}}$ for the three targets are presented in fig. 4. The integrals decrease with Q^2 and remain

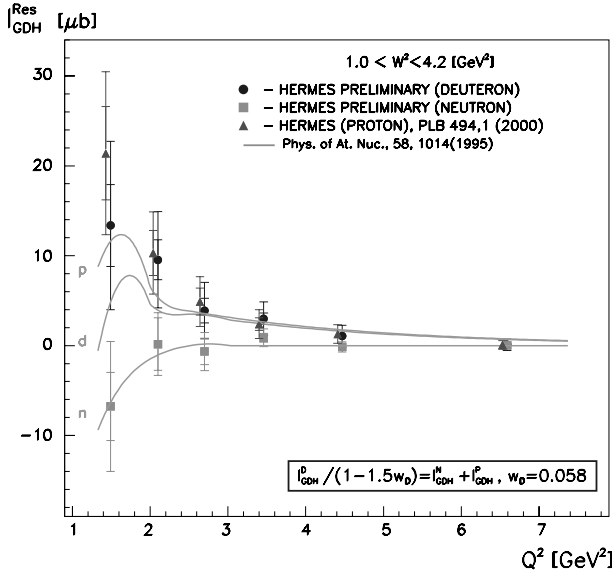


Fig. 3. Results for the generalised GDH integrals in the resonance region.

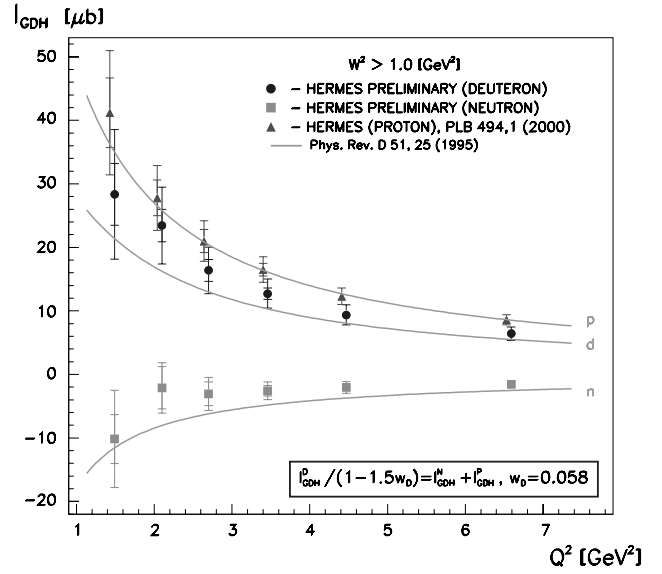


Fig. 5. Results for the generalised GDH integrals.

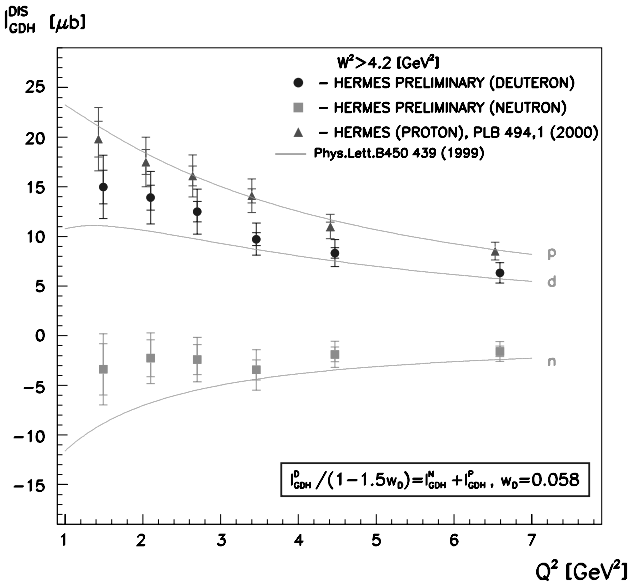


Fig. 4. Results for the generalised GDH integrals in the DIS region.

sizeable even at the lowest measured Q^2 . Data with $Q^2 > 3 \text{ GeV}^2$ are in agreement with the multiple-Reggeon exchange parameterisation [21] for the cross-section difference used for the extrapolation into the unmeasured region for $W^2 > 45 \text{ GeV}^2$.

The results of the total I_{GDH} integrals in the full W^2 range are presented in fig. 5. Data are compared to a model based [22] on the leading-twist Q^2 evolution of the first moments of the two polarised structure functions g_1 and g_2 , without considering any explicit nucleon resonance contribution. The statistical and systematic uncertainties of the full I_{GDH} are clearly dominated by the uncertainties in the nucleon resonance region. They are particularly large due to the smallness of D and the large size of η ac-

centuating the uncertainties in A_2^d , which amounts to 30% of the nucleon resonance contribution. The systematic uncertainty on A_2^d in the DIS region does not contribute significantly. The systematic uncertainty for the extrapolation to the unmeasured region at high W^2 of 5% has been taken into account. The experimental data are consistent with the naive expectation that the $1/Q^2$ expansion is a good approximation down to $Q^2 \simeq 2 \text{ GeV}^2$. In principle, the elastic part at $x = 1$ has to be included for a complete comparison to a twist expansion of Γ_1 ; however, this is not a relevant contribution in the kinematic range considered. There is no observed sign change in the measured range that would be required for the generalised GDH integral on the proton or the deuteron to meet the negative GDH sum rule predictions at $Q^2 = 0$.

4 Summary

In conclusion, the first experimental evidence of quark-hadron duality for the polarised structure function g_1 on the proton has been presented for Q^2 values larger than 1.7 GeV^2 . The spin asymmetries measured in the nucleon resonance region have been found to be in agreement with the spin asymmetries measured in the DIS region at larger W^2 . This experimental finding indicates that the description of the spin asymmetry in terms of quark degrees of freedom is valid also in the nucleon resonance region within the kinematic range probed by the present experiment. The quark-hadron duality for the polarised structure function g_1 has been found satisfied at a similar Q^2 as for the unpolarised structure function F_2 .

The Q^2 -dependence of the GDH integral for the proton, neutron and deuteron is also given, evaluating separately the contributions of the nucleon resonance and deep inelastic regions: the latter has been found to be dominant for $Q^2 > 3 \text{ GeV}^2$, while both contributions are

important at low Q^2 . The total integrals show no significant deviation from the $1/Q^2$ behavior in the measured Q^2 range, and thus no sign of large effect due to either nucleon resonance excitations or non-leading twists. The strong turn-down of generalised GDH integrals for proton and deuteron towards the real-photon prediction should occur at Q^2 lower than 1.2 GeV^2 .

References

1. E.D. Bloom, F.J. Gilman, Phys. Rev. Lett. **25**, 1140 (1970); Phys. Rev. D **4**, 290 (1971).
2. A. De Rujula, H. Georgi, H.D. Politzer, Phys. Lett. B **64**, 428 (1976); Ann. Phys. **103**, 315 (1977).
3. N. Isgur *et al.*, Phys. Rev. D **64**, 054005 (2001).
4. I. Niculescu *et al.*, Phys. Rev. Lett. **85**, 1186 (2000).
5. F. Close, N. Isgur, Phys. Lett. B **509**, 811 (2001); V.D. Burkert, B.L. Ioffe, J. Exp. Theor. Phys. **78**, 619 (1994).
6. C.E. Carlson, N.C. Mukhopadhyay, Phys. Rev. D **58**, 94029 (1998).
7. S.B. Gerasimov, Sov. J. Nucl. Phys. **2**, 430 (1966); S.D. Drell, A.C. Hearn, Phys. Rev. Lett. **16**, 908 (1966).
8. F.J. Gilman, Phys. Rev. **167**, 1365 (1968).
9. HERMES Collaboration (K. Ackerstaff *et al.*), Nucl. Instrum. Methods A **417**, 230 (1998).
10. S.I. Bilen'kaya *et al.*, Zh. Eksp. Teor. Fiz. Pis'ma **19**, 613 (1974).
11. A. Bodek, *et al.*, Phys. Rev. D **20**, 1471 (1979).
12. NMC Collaboration (P. Amaudruz *et al.*), Phys. Lett. B **364**, 107 (1995).
13. E143 Collaboration (K. Abe *et al.*), Phys. Rev. D **58**, 112003 (1998).
14. HERMES Collaboration (A. Airapetian *et al.*), Phys. Rev. Lett. **90**, 092002 (2003), hep-ex/0209018.
15. L.W. Whitlow *et al.*, Phys. Lett. B **250**, 193 (1990).
16. O. Nachtmann, Nucl. Phys. B **63**, 237 (1973).
17. HERMES Collaboration, Phys. Lett. B **444**, 531 (1998).
18. HERMES Collaboration, Phys. Lett. B **494**, 1 (2000).
19. M. Lacombe *et al.*, Phys. Lett. B **101**, 139 (1981).
20. I.G. Aznauryan, Phys. At. Nucl. **58**, 1014 (1995).
21. N. Bianchi, E. Thomas, Phys. Lett. B **450**, 439 (1999).
22. J. Soffer, O.V. Teryaev, Phys. Rev. D **51**, 25 (1995); Phys. Rev. Lett. **70**, 3373 (1993).